

# Chapter 6

## Polymer Nanocomposites for Power Energy Storage

Qi Li and Qing Wang

### 6.1 Introduction

Dielectric capacitors that store electric energy through static charge separation between two opposite electrodes induced by the external electric field are ubiquitous in electronics and electric power systems. When a dielectric capacitor is connected to a charging circuit, the amount of electric energy per volume that can be stored in dielectric capacitors is called stored energy density, and when the charged capacitor is then connected to a discharging circuit, the amount of energy per volume that can be released is called dischargeable energy density. These energy densities are usually measured volumetrically in joule per cubic centimeter ( $\text{J}/\text{cm}^3$ ).

Energy density is one of the most important criteria for energy storage devices. While dielectric capacitors bear the intrinsic advantage of fast charge and discharge, the energy densities of commercially available dielectric capacitors are much lower relative to their electrochemical counterparts, such as batteries and electrochemical capacitors [1–4]. As the energy density of capacitors is governed by the dielectric materials that separate the opposite static charges between two electrodes, the development of dielectric materials with greatly improved energy density has thus been a major enabling technology for high-energy-density dielectric capacitors.

In general, to compute the energy density of a dielectric material, electric displacement ( $D$ ) of the material is measured as a function of electric field ( $E$ ) during the charge–discharge process to plot the  $D$ - $E$  loop (Fig. 6.1). The stored energy density is equal to the integral

$$U_s = \int E dD \quad (6.1)$$

---

Q. Li, PhD • Q. Wang, PhD (✉)

Department of Materials Science and Engineering, The Pennsylvania State University,  
University Park, State College, PA 16802, USA

e-mail: [qul14@psu.edu](mailto:qul14@psu.edu); [wang@matse.psu.edu](mailto:wang@matse.psu.edu)

where  $E$  is the electric field and  $D$  is the electric displacement. As shown in Fig. 6.1, the area of the region that is bounded by the graph of charging, the  $D$ -axis, and the horizontal line  $y=D_{max}$  defines the stored energy density. Similarly, the area of the region that is bounded by the graph of discharging, the  $D$ -axis, and the horizontal line  $y=D_{max}$  defines the dischargeable energy density ( $U_d$ ). The dissipated energy ( $U_l$ ) caused by electric conduction and/or ferroelectric hysteresis is indicated by the region surrounded by the loop. Apparently, the total charged energy density ( $U_s$ ) is equal to  $U_d$  plus  $U_l$ . The charge–discharge efficiency ( $\eta$ ) is defined as  $U_d/U_s \times 100\%$ . In particular, for linear dielectrics, the stored energy density can be simply calculated following the equation:

$$U_s = \frac{1}{2} DE = \frac{1}{2} \epsilon_r \epsilon_0 E^2 \quad (6.2)$$

where  $\epsilon_r$  is the relative static permittivity,  $\epsilon_0$  is the permittivity of free space, and  $E$  is the applied electric field.

Equations 6.1 and 6.2 together suggest that the energy density of a dielectric could be improved by increasing at least one of the two parameters, i.e., the dielectric constant ( $K$ ) and the electric breakdown strength ( $E_b$ ). This is because  $K$  determines the electric displacement, and  $E_b$  defines the highest field that can be applied on the dielectric. Recently, to integrate the complementary advantages of inorganic and organic dielectric materials for high energy storage, attempts to incorporate inorganic nanoparticles with high  $K$  into polymer matrices have been made via mechanical blending, solution mixing, or in situ radical polymerization [5–12]. This chapter summarizes the recent progress in polymer nanocomposites for dielectric power energy storage.

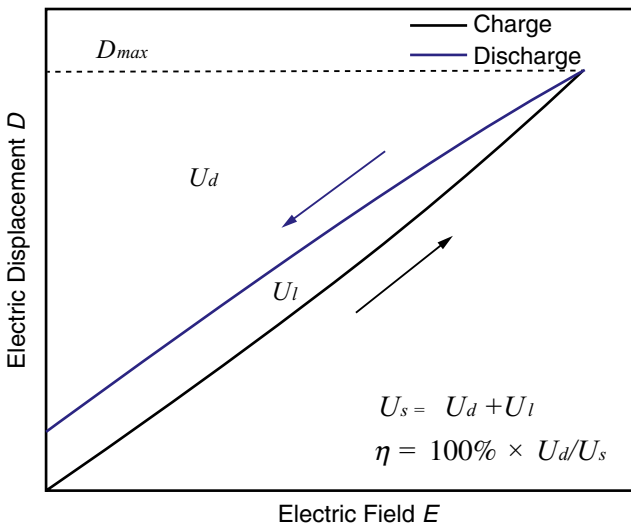


**Fig. 6.1** Schematic  $D$ - $E$  loop for a dielectric material

## 6.2 Increasing Dielectric Constant of Polymer Nanocomposites

Inorganic materials, such as the barium titanate, enjoy very high- $K$  values (typically ranging from thousands to hundreds of thousands) but are limited by the low  $E_b$  (i.e., lower than 100 MV/m) [13]. On the other hand, polymer dielectrics possess good processability, low cost, light weight, high  $E_b$ , and graceful failure, although their  $K$  values are much lower than those of their inorganic counterparts [14–16]. For example, one of the best commercially available polymer dielectrics, represented by the biaxially oriented polypropylenes (BOPP), has a  $K$  of  $\sim 2.2$ , and an  $E_b$  of  $> 700$  MV/m [17]. As a result, at comparable electric fields, inorganic dielectrics show much higher energy densities in comparison to organic dielectrics. It is thus a promising strategy to incorporate inorganic nanoparticles into polymer dielectrics to increase the effective dielectric constant of the composite material and, at the mean time, preserve the high breakdown strength of the polymer.

### 6.2.1 Using Ceramics as Fillers

The effective dielectric constant of a two-phase composite system can be predicted by the Maxwell Garnett equation on the basis of the effective medium theory that can be expressed as [18]

$$\varepsilon = \varepsilon_2 \frac{2\varphi_1(\varepsilon_1 - \varepsilon_2) + \varepsilon_1 + 2\varepsilon_2}{2\varepsilon_2 + \varepsilon_1 + \varphi_1(\varepsilon_2 - \varepsilon_1)} \quad (6.3)$$

where  $\varepsilon$  is the effective permittivity of the composite and  $\varphi_1$  and  $\varphi_2$  are the volume fractions of filler phase and polymer phase, which have relative permittivities of  $\varepsilon_1$  and  $\varepsilon_2$ , respectively. Equation 6.3 indicates that the incorporation of high- $K$  fillers would directly give rise to an increased  $K$  value of the composite material. Besides, the coupling effect occurring at the interface areas in the nanocomposite would create considerable level of interfacial polarization between the filler and matrix phases that advances the energy density of the material [19–21]. Indeed, experimental results have shown that much increased  $K$  values of the polymer nanocomposites are attained with high- $K$  inclusions such as  $\text{BaTiO}_3$ ,  $\text{Ba}_x\text{Sr}_{1-x}\text{TiO}_3$ ,  $\text{CaCu}_3\text{Ti}_4\text{O}_{12}$ , and  $\text{Pb}(\text{Zr}, \text{Ti})\text{O}_3$ , leading to improved energy densities [22–46].

#### 6.2.1.1 Surface Functionalization of Filler Particles

Since nanoscale fillers possessing large surface areas could provide high levels of interfacial polarization, they are the inclusions of the choice for dielectric polymer composites with high energy densities. Because nanoparticles have strong tendency

to aggregate in a polymer matrix due to the high surface energy, they are usually surface functionalized in order to improve the compatibility and achieve homogeneous distributions. This is beneficial in two aspects: (1) uniform dispersion of high- $K$  fillers would minimize the degree of distortion of the local field induced by the large difference in dielectric constant between the filler and matrix phases [47] and (2) elimination of filler aggregation could get rid of the microstructural defects at the filler–matrix interface such as voids and flaws. This is important as either the distortion of the local field or the microstructural defects would result in a significant decrease in breakdown strength of the nanocomposite and thereby offset any potential gain in the energy density from increased  $K$  values.

Perry et al. reported phosphonic acid-modified BaTiO<sub>3</sub>–polymer nanocomposites and concluded that the use of particles modified with suitable phosphonic acid ligands leads to well-dispersed BaTiO<sub>3</sub> nanocomposite films with high dielectric constant [25]. The authors examined a series of ligands as the modifier, each bearing an aliphatic octyl chain with a different terminal binding group. It was found that the ligand bearing the phosphonic acid functional group could be firmly bound on BaTiO<sub>3</sub> nanoparticles in a tridentate form. To demonstrate the effectiveness of the proposed strategy, the authors provided two examples using these ligands (Fig. 6.2a) to modify BaTiO<sub>3</sub> nanoparticles, and two polymer dielectrics were chosen as matrices, i.e., the bisphenol-A-type polycarbonate (PC) and the poly(vinylidene fluoride-co-hexafluoropropylene) (P(VDF-HFP)). The obtained nanocomposites showed much higher  $K$  values relative to the blank polymers and fairly low dielectric loss (Fig. 6.2b), even though the breakdown strength was also relatively low (~210 MV/m) compared with those of the polymer matrices (e.g.,  $E_b$  of the P(VDF-HFP) is around 500 MV/m). As a result, the stored energy densities were improved, i.e., 3.9 J/cm<sup>3</sup> for the BaTiO<sub>3</sub>–PC nanocomposite and 6.1 J/cm<sup>3</sup> for the BaTiO<sub>3</sub>–P(VDF-HFP) nanocomposite. Following this strategy, a variety of ligands were developed to modify the high- $K$  ceramics for dielectric polymer nanocomposites, such as ethylene diamine [23], dopamine [33], organic titanate coupling agent [44], and silane coupling agent [45, 46].

Another approach to improving the dispersion of filler particles is to directly link the nanoparticles to the molecular chain of the host matrices via covalent bonding. This can be achieved through two different methods which are coined as “grafting from” [48–51] and “grafting to” [26, 30, 52–54] methods, respectively.

The so-called “grafting from” method is referred to describe the initialization of the growth of polymer chains from the surface of nanoparticles. Marks et al. proposed an in situ synthesis of high-energy-density metal oxide nanocomposites [48]. The dielectric nanocomposites were prepared via in situ metallocene polymerization of isotactic propylene from the surface of methylaluminoxane (MAO)-coated inorganic nanofillers (Fig. 6.3). The authors first anchored the MAO onto the nanoparticles via surface hydroxyl group reaction to form covalent Al–O bonds. Then anchored MAO functioned as a co-catalyst to activate the metallocene, and in addition, the hydrophobic MAO functionalization helped disrupt, in combination with ultrasonication, hydrophilic nanoparticle agglomeration in the hydrophobic reaction medium. In virtue of the covalent linkage between the filler and matrix phases, uniform filler distribution was attained in the as-prepared nano-

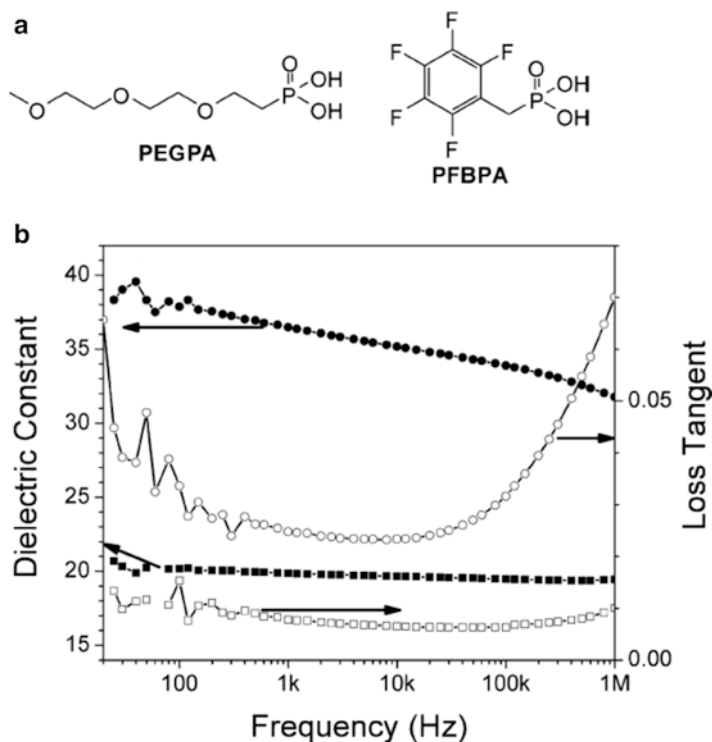


**Fig. 6.2** (a) Molecular structures of phosphonic acid ligands used to modify BaTiO<sub>3</sub> nanoparticles. (b) Frequency-dependent dielectric response of capacitor devices fabricated from PEGPA-BT/PC (*squares*) and PFBPA-BT/P(VDF-HFP) (*circles*) (Reprinted from Ref. [25] with permission from John Wiley and Sons)

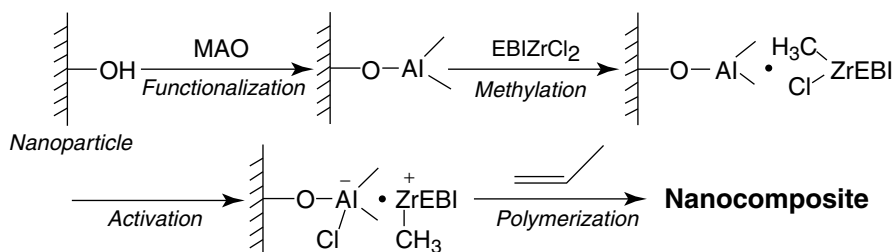


**Fig. 6.3** Schematic illustration of synthetic route of isotactic polypropylene-metal oxide nanocomposites (Reprinted with permission from Ref. [48]. Copyright 2007 American Chemical Society)

composites that exhibited moderately increased dielectric constant with high breakdown strength of the polymer matrix being maintained. Consequently, the energy density of the nanocomposite was calculated to be as high as 9.4 J/cm<sup>3</sup>. This approach was then extended to other types of polymer matrices by employing different chemistry and polymerizing techniques. For example, Jiang et al. devel-

oped a BaTiO<sub>3</sub>–poly(methyl methacrylate) (PMMA) nanocomposite that was prepared by in situ atom transfer radical polymerization (ATRP) of methyl methacrylate (MMA) from the surface of BaTiO<sub>3</sub> nanoparticles (Fig. 6.4) [49]. By doing so, the dielectric constant of the nanocomposite was improved to ~14.6 from 3.5 of the pure polymer, and in the meantime, the dielectric loss was almost independent of the filler content.

The “grafting to” method involves establishing covalent binding between the filler and polymer phases through functional groups on the polymer chains and the surface of filler particles. A typical example was reported by Wang and coworkers [27]. They prepared the ferroelectric polymers with phosphonic acid end groups (Fig. 6.5a) and subsequently used the reactive terminal groups of the polymer for direct coupling with oxide fillers. The formation of covalent coupling between the polymer matrix and filler particles renders the nanocomposites with good stability and uniform filler dispersion (Fig. 6.5b). Due to the rise of the electric displacement induced by the incorporated nanofillers, the energy storage capability of the nanocomposites was improved (Fig. 6.5c). Another example of the “grafting to” method introduced glycidyl methacrylate (GMA) functionalized P(VDF-HFP) as the matrix to accommodate BaTiO<sub>3</sub> nanoparticles, and the covalent linking of the matrix and filler phases was achieved via ring-opening reaction between the epoxy groups of GMA grafted onto P(VDF-HFP) and the amino groups on the surface of BaTiO<sub>3</sub> nanoparticles (Fig. 6.6a) [52]. Again, homogeneous filler dispersion and improved dielectric constant were observed in the nanocomposites (Fig. 6.6b, c).

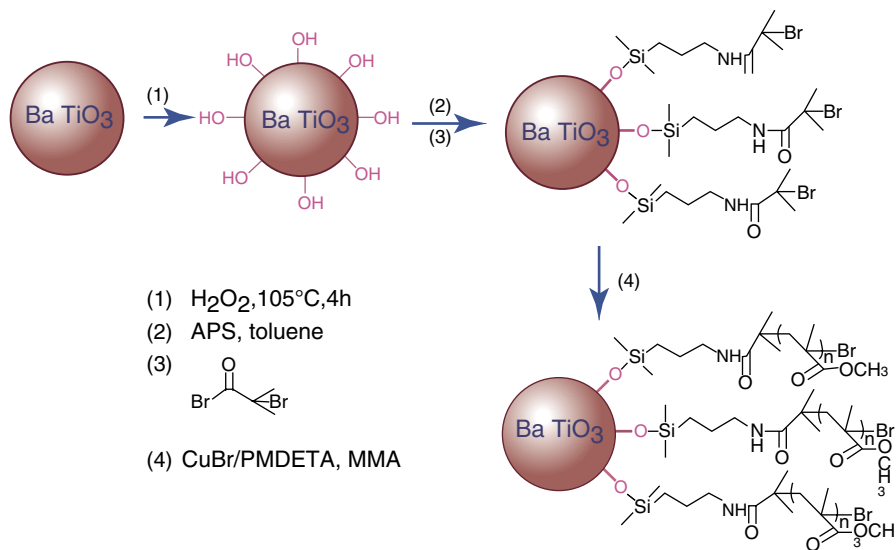


**Fig. 6.4** Schematic diagram illustrating the process of ATRP from the surface of BaTiO<sub>3</sub> (Reprinted from Ref. [49] with permission from Royal Society of Chemistry)

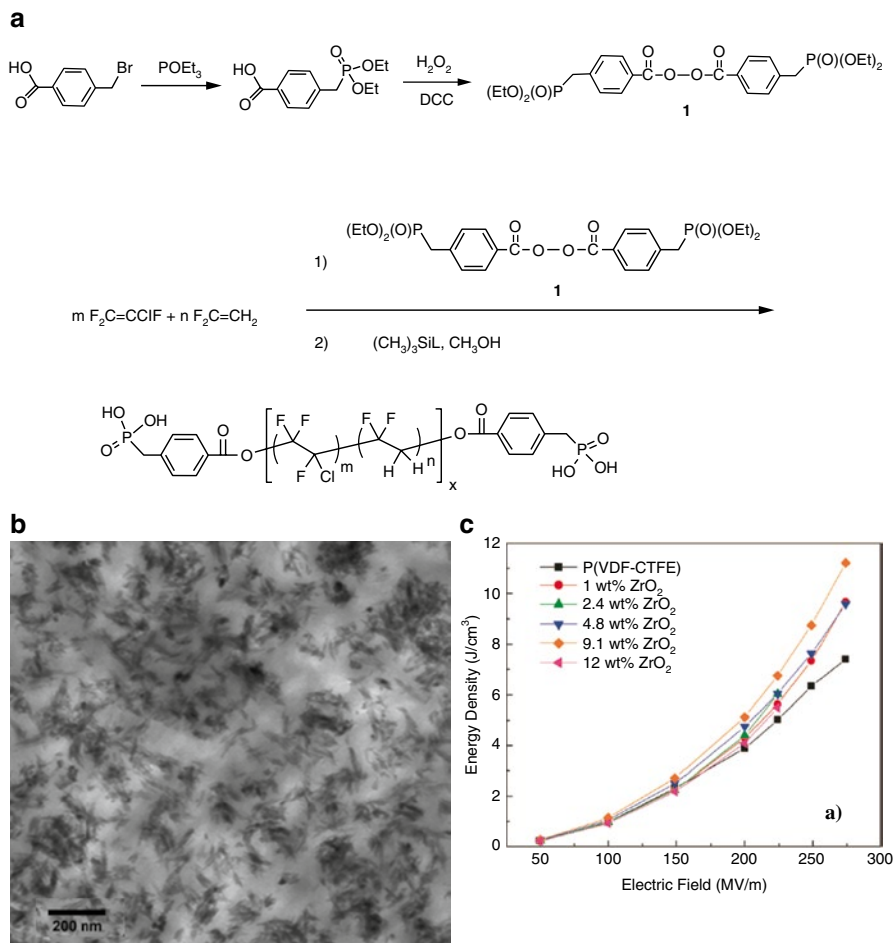


**Fig. 6.5** (a) Synthesis of the functional initiator and the phosphonic acid-terminated P(VDF-CTFE). (b) TEM image of the covalently bonded P(VDF-CTFE). (c) Stored energy density of the polymer and the nanocomposites as a function of the applied field (Reprinted with permission from Ref. [27]. Copyright 2010 American Chemical Society)

### 6.2.1.2 High Aspect Ratio Fillers

Three-dimensional continuous polymer matrices filled with zero-dimensional nanoparticles is usually referred to as 0-3 polymer nanocomposites. Similarly, those containing one-dimensional inclusions are 1-3 polymer nanocomposites. Recent studies on dielectric nanocomposites have shown that high- $K$  nanofillers with high aspect ratios, i.e., one-dimensional nanowires or nanorods, could lead to more significant increase in dielectric constant of dielectric polymers, as compared with zero-dimensional nanoparticles [40, 55–58]. Therefore, composing 1-3 polymer nanocomposites has become a promising strategy toward high-energy-density capacitors.

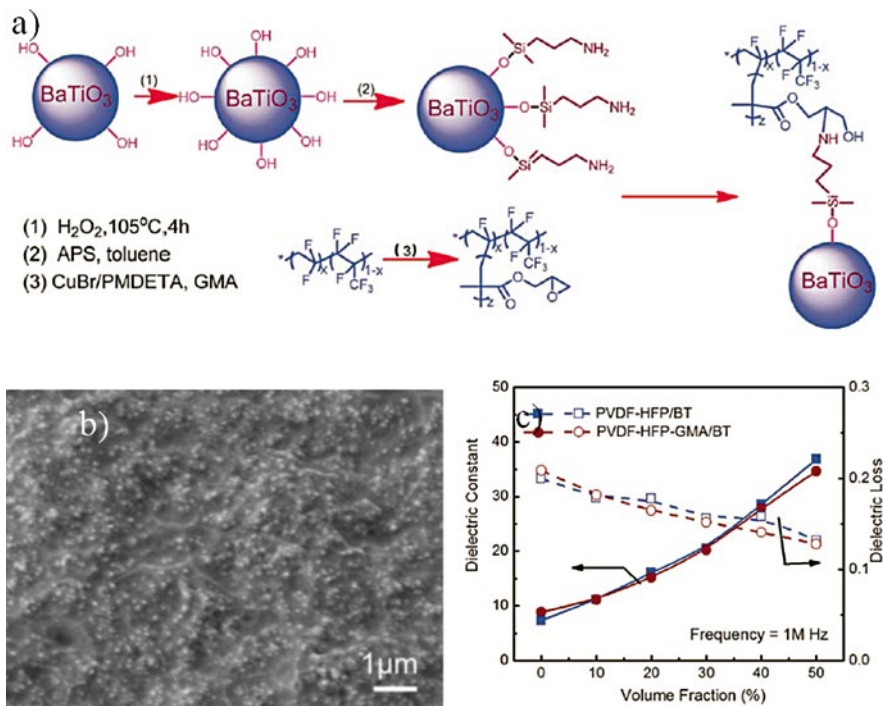


**Fig. 6.6** (a) Schematic illustration of the preparation process for the PVDF-HFP-GMA–BT nanocomposites. (b) SEM images of the fractured surface of the PVDF-HFP-GMA nanocomposite with 20 vol%  $\text{BaTiO}_3$  nanoparticles. (c) Comparison of the dielectric properties for the PVDF-HFP-GMA–BT and PVDF-HFP–BT nanocomposites at 1 MHz (Reprinted from Ref. [52] with permission from Royal Society of Chemistry)

Sodano et al. reported lead zirconate titanate (PZT)–polyvinylidene fluoride (PVDF) dielectric nanocomposites, in which the nanosized inclusions were of different aspect ratios and are termed as nanowires (higher aspect ratio) and nanorods (lower aspect ratio), respectively [40]. The nanocomposite filled with PZT nanowires showed higher dielectric constant and lower loss than that loaded with PZT nanorods, which gave rise to a higher energy density, demonstrating the effectiveness of using high aspect ratio nanofillers for the fabrication of polymer nanocomposites for capacitive energy storage.

By using  $\text{BaTiO}_3$  nanowires as the filler, the energy density of a ferroelectric terpolymer poly(vinylidene fluoride-trifluoroethylene-chlorofluoroethylene) (P(VDF-TrFE-CFE)) was increased by 45 %, achieving 10.48 J/cc at the electric field of 300 MV/m [55]. Later,  $\text{Ba}_{0.2}\text{Sr}_{0.8}\text{TiO}_3$  nanowires were also employed to prepare a composite dielectric using PVDF as the matrix (Fig. 6.7) [56]. The discharged energy density of the nanocomposite, namely, 14.86 J/cc, was 43 % larger relative to the pure PVDF, which was attained at the electric field of 450 MV/m (Fig. 6.8). Because polymer dielectrics filled with high- $K$  nanowires can achieve higher dielectric



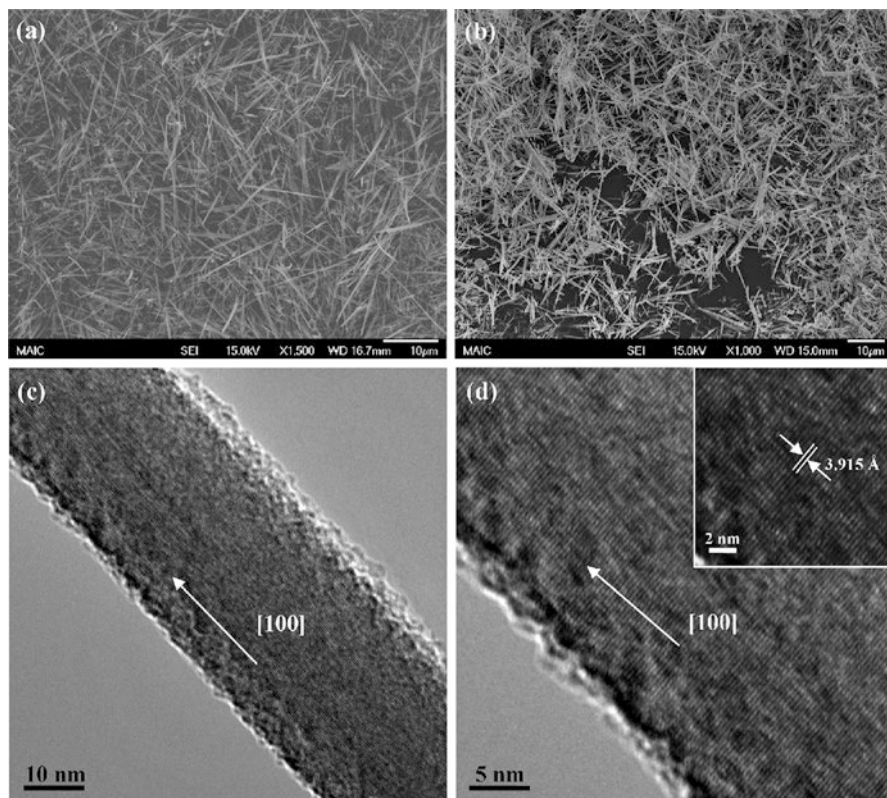


**Fig. 6.7** SEM images of (a) sodium titanate NWs and (b)  $\text{Ba}_{0.2}\text{Sr}_{0.8}\text{TiO}_3$  NWs. (c) TEM image of a single  $\text{Ba}_{0.2}\text{Sr}_{0.8}\text{TiO}_3$  nanowire. (d) Representative HRTEM image showing clear crystal lattice fringes of the  $\text{Ba}_{0.2}\text{Sr}_{0.8}\text{TiO}_3$  nanowire (Reprinted with permission from Ref. [56]. Copyright 2013 American Chemical Society)

constants than those filled with high- $K$  nanoparticles, lower filler content is required for 1-3 systems to induce a similar level of electric displacement as compared with the 0-3 system. This would naturally result in a higher breakdown strength for the 1-3 nanocomposite since breakdown strength decreases with increasing feeding ratio of the high- $K$  fillers.

### 6.2.1.3 Nanofillers with Moderate Dielectric Constant

According to the Maxwell Garnett equation (Eq. 6.3), high- $K$  nanofillers would be the dopants of choice for improving the dielectric constant of polymer dielectrics. However, the presence of high- $K$  nanofillers in dielectric polymers causes highly inhomogeneous electric field across the nanocomposite due to the large

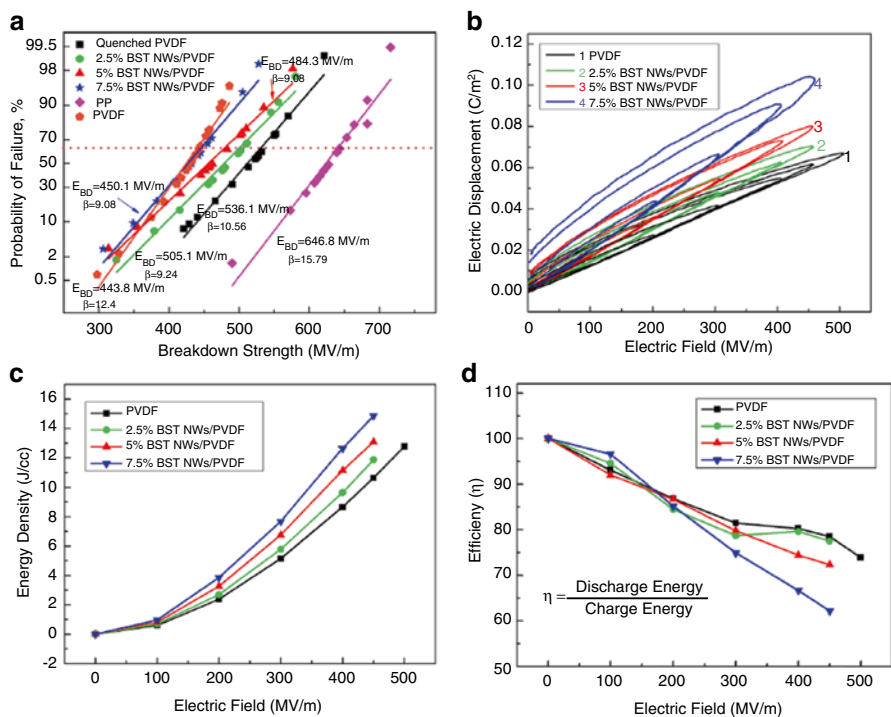


**Fig. 6.8** (a) Weibull distribution and observed dielectric breakdown strength of nanocomposites with different volume fraction of BST, quenched PVDF, untreated PVDF, and commercial polypropylene films; (b) unipolar electric  $D$ - $E$  loops for nanocomposites with different BST NWs volume fractions; (c) energy density of the nanocomposite with different volume fraction as a function of the electric field calculated from  $D$ - $E$  loops; (d) efficiencies of the nanocomposites with different volume fraction as a function of the electric field (Reprinted with permission from Ref. [56]. Copyright 2013 American Chemical Society)

contrast in dielectric constant between the dopant and matrix phases, which drastically decreases the breakdown strength of the composite system [47]. But what if nanofillers with moderate dielectric constant are used as dopants to fabricate dielectric nanocomposites?

To answer this question, Wang et al. proposed a new type of nanocomposites with comparable dielectric constants between the filler and matrix phases, i.e.,  $K=42$  for the host ferroelectric terpolymer poly(vinylidene fluoride-*ter*-trifluoroethylene-*ter*-chlorotrifluoroethylene) (P(VDF-TrFE-CTFE)) and  $K=47$  for the fillers ( $\text{TiO}_2$  nanocrystals) [22]. Interestingly, the polarization of the nanocomposite was found to be significantly enhanced despite of the moderate dielectric constant of the nanofillers involved. The unexpected improvement in polarization was attributed to the large interfacial polarization, which was supported by the results of temperature dependent dielectric spectroscopy showing an emerging dielectric anomaly (Fig. 6.9). As a result of the enhanced polarization, the energy

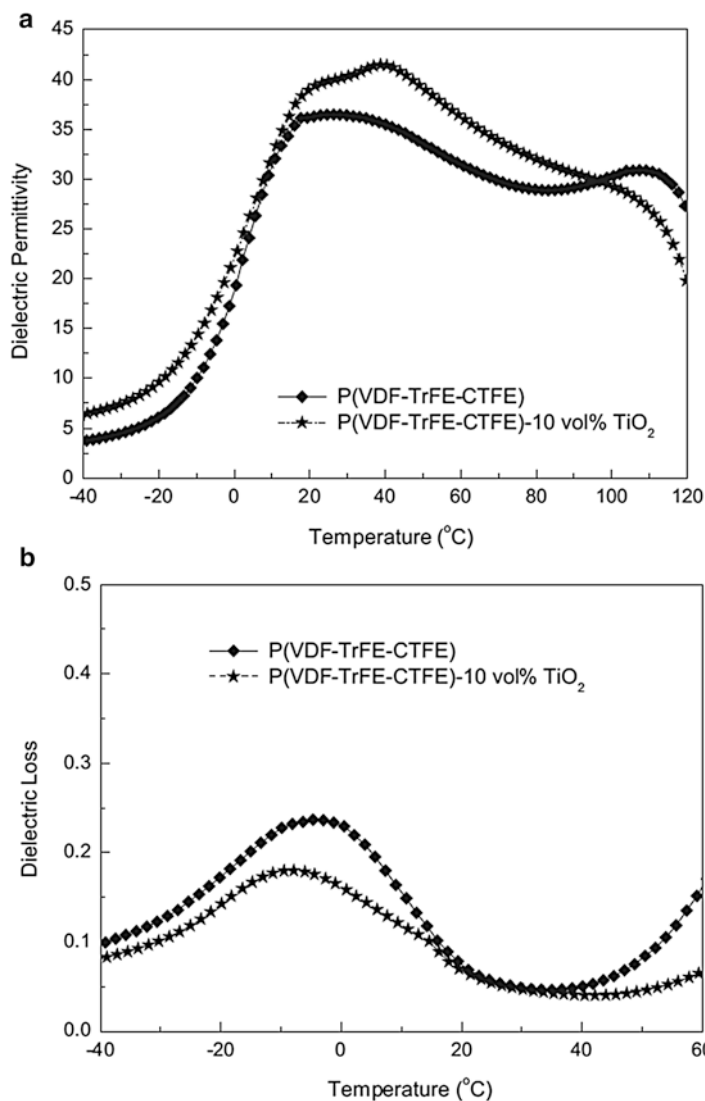


**Fig. 6.9** Temperature dependence of the (a) dielectric constant and (b) dielectric loss of the polymer and nanocomposite measured at 1 kHz (Reprinted from Ref. [22] with permission from John Wiley and Sons)

density of the nanocomposite was found to be 40 % higher than that of the pristine terpolymer under an electric field of 200 MV/m. By employing nanofillers with moderate dielectric constant, the polarization could be increased without compromising breakdown strengths of host polymers and thus leading to much improved capacitive energy storage capabilities. Along this line, polymer nanocomposites

incorporating other nanofillers with moderate dielectric constant were also studied [12, 27, 59–66]. The success of this approach suggests that the usage of high- $K$  nanofillers may not be necessary for producing high-energy-density dielectric polymer nanocomposites.

## 6.2.2 Percolative Polymer Nanocomposites

Percolation theory predicts that in the conductive particle–polymer composite system, dielectric constant increases sharply as the filler content increases to the vicinity of the percolation threshold, which can be expressed by

$$\frac{K}{K_m} = \left| \frac{f_c - f_{fil}}{f_c} \right|^{-q} \quad (6.4)$$

where  $K$  is the dielectric constant of the composite,  $K_m$  is the dielectric constant of the polymer matrix,  $f_c$  is the percolation threshold, and  $f_{fil}$  is the filler content [67]. Such abrupt increase in dielectric constant is ascribed to the formation of the so-called microcapacitor networks consisting of a large number of local capacitors [19]. Each of these microcapacitors is formed by the neighboring conductive particles as the two electrodes and a thin layer of dielectric polymer in between. All these microcapacitors contribute to the intensified local electric fields and consequently result in accumulation of charge carriers at the filler–matrix interface responsible for the increased interfacial polarization.

### 6.2.2.1 Giant Dielectric Constants of Percolative Nanocomposites

By capitalizing on the percolation strategy, numerous percolative polymer composites have been prepared incorporating various conductive fillers including zero-dimensional nanoparticles [68–76], one-dimensional nanotubes [77–88] and nanofibers [89–92], as well as two-dimensional nanoplates [93–98], and all show giant dielectric constants in the neighborhood of the percolation thresholds. For example, Nan et al. reported nickel particles filled polymer composites, in which drastic increase in dielectric constant was observed near the percolation threshold, i.e., from 10 of the host polymer to 400 of the composite with 17 vol.% of conductive fillers [70]. Dang et al. developed carbon nanotube–PVDF percolative polymer nanocomposites that displayed high dielectric constant of 300 at low filler content (2 vol.%) due to the low percolation threshold (1.61 vol.%) [78]. Fan et al. described a sort of percolative composites incorporating exfoliated graphite nanoplates (xGNPs) [93]. At 2.34 vol.% feeding of the xGNPs, the dielectric constant reached as high as  $4.5 \times 10^7$  (Fig. 6.10).

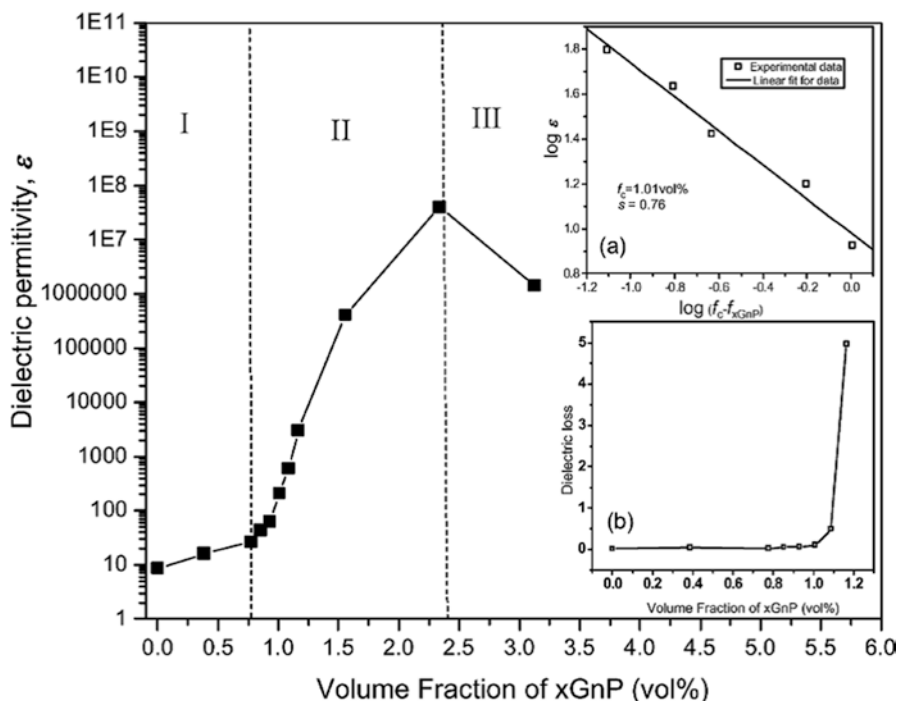


**Fig. 6.10** Effective dielectric constant of the PVDF-xGnP nanocomposites as a function of the xGnP volume fraction, measured at 1000 Hz and room temperature. Inset (a) shows the best fits of the conductivity to Eq. 6.2. Inset (b) shows the loss tangent of PVDF-xGnP nanocomposites as a function of xGnP volume fraction (Reprinted from Ref. [93] with permission from John Wiley and Sons)

### 6.2.2.2 Conductive Fillers Covered with Insulation Layer

Although much increased dielectric constants have been observed in percolative polymer nanocomposites, the high conduction losses of these materials associated with the involved conductive fillers hindered their applications in power energy storage due to the low breakdown strength. To circumvent this problem, a plenty of efforts have focused on the creation of an insulation layer on the surface of conductive fillers to avoid the formation of conducting pathways. For instance, Nan et al. put forward a strategy using core-shell structured nanofillers with metal particle cores and organo carbon shells (Fig. 6.11) [75]. The presence of the shell structure prevented the conductive metal particles from directly connecting with each other and thus lead to a low dielectric loss ( $\sim 3\%$ ) even at percolation threshold.

Wang et al. prepared a poly(vinylidene fluoride-co-chlorotrifluoroethylene) (P(VDF-CTFE))-based percolative nanocomposite using  $\text{SiO}_2$ -coated graphene nanosheets as fillers and studied the dielectric properties at both weak and high fields [95]. While they found a fairly low dielectric loss even beyond the percolation

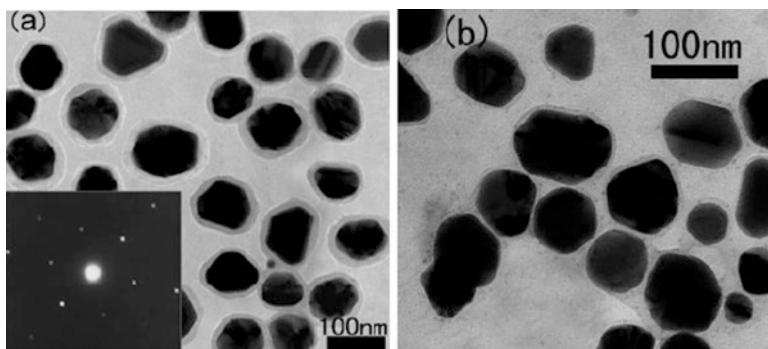


**Fig. 6.11** TEM of the Ag–C core-shell particles with (a) thicker shells and (b) thinner shells (not as clearly visible as the thicker shells), where the inset in (a) shows the selected area electron diffraction pattern of the particles, indicating that the Ag cores are single Ag crystals (Reprinted from Ref. [75] with permission from John Wiley and Sons)

threshold, a relatively high dielectric strength was also observed, both of which were attributed to the uniform coating of insulation layer on the surface of graphene nanosheets (Fig. 6.12). Marks et al. used metallic aluminum nanoparticles with a native insulation layer of aluminum oxide as fillers to compose the percolative nanocomposite [76]. Due to the very high dielectric constant achieved and preserved breakdown strength, the energy density was calculated to be as high as  $14.4 \text{ J/cm}^3$ .

### 6.3 Increasing Breakdown Strength of Polymer Nanocomposites

In linear dielectrics,  $U_s$  scales quadratically with  $E$  and linearly with  $K$ . A high  $E$  is more profitable than a high  $K$  for achieving high energy density of dielectric materials. As  $E_b$  signifies the maximum  $E$  that can be applied on a dielectric material,  $E_b$  becomes the very critical parameter that determines the  $U_s$  of dielectric materials. One example is that although the  $K$  value ( $\sim 2.2$ ) of BOPP is 100–1000 times lower than those (usually at the level of  $10^3$ – $10^4$ ) of typical dielectric ceramics, such as barium titanate, they share a very similar  $U_s$  of  $\sim 5 \text{ J/cm}^3$ , owing to the superior  $E_b$  of BOPP (700 MV/m) compared to that of the ceramic films, i.e.,  $\sim 90 \text{ MV/m}$ . For these reasons, efforts have been made in developing high- $E_b$  polymer dielectrics using the composite approach [99–103].

#### 6.3.1 Polymer Nanocomposites with Insulating Nanoparticles

Roy et al. are among the first to observe the improved dielectric strength from insulating nanoparticle-filled polymer composites. They found that XLPE filled with vinylsilane-treated silica nanoparticles had a much higher Weibull

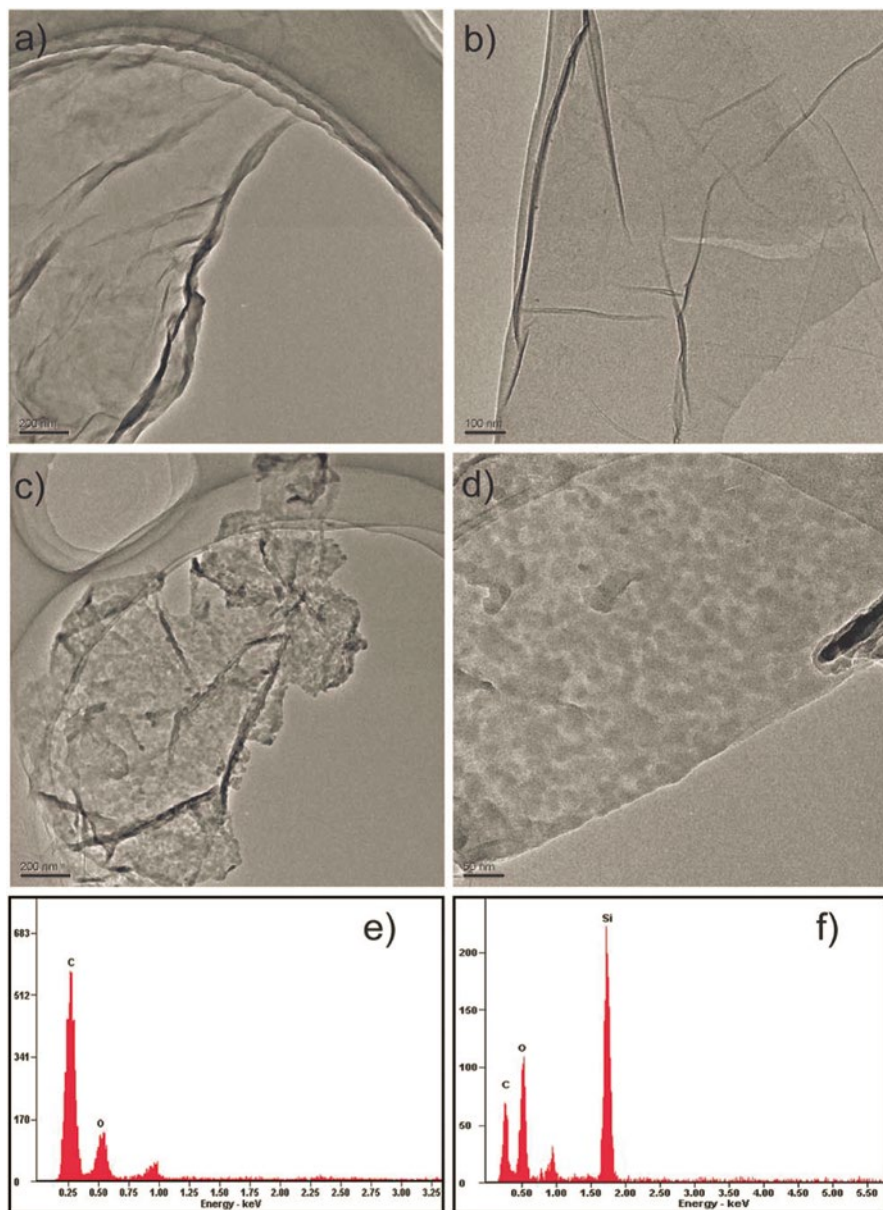


**Fig. 6.12** TEM images of (a, b) GO and (c, d) r-GO-SiO<sub>2</sub>, and EDX analysis of (e) GO and (f) r-GO-SiO<sub>2</sub>. Scale bar: (a) 200 nm, (b) 100 nm, (c) 200 nm, and (d) 50 nm (Reprinted from Ref. [95] with permission from Royal Society of Chemistry)

breakdown strength than the bare polymer, i.e.,  $\sim 500$  MV/m vs.  $\sim 300$  MV/m [99]. The authors claimed that physical bonding between nanoparticles and the polymer chain could account for the increase in breakdown strength. Takala et al. then studied silica nanoparticle-filled dielectric composites by use of PP as the matrix [100]. The as-prepared nanocomposites exerted significantly improved breakdown strength relative to the blank polymer. It was believed that the breakdown strength results related to scattering and reduced space charge accumulation, which had an effect on both ac and dc behaviors of the nanocomposite. Nano-dispersion of silica also ensured low loss factor of the nanocomposite, which was owing to the large fraction of interface volume and polymer chain entanglement keeping the motion of charge carriers limited.

### 6.3.2 Incorporation of Insulating Nanolamillates

More recently, it was demonstrated that incorporation of two-dimensional insulating nanostructures in dielectric polymers could lead to essentially increased breakdown strength [101–103].

In a P(VDF-HFP)-based polymer nanocomposite, high aspect ratio two-dimensional kaolinite clays were employed as fillers [101]. The composite films were first cast from solution and then hot-pressed at  $200$  °C and  $55$  MPa pressure. After cooling in air, the films were uniaxially stretched mechanically by means of a zone drawing process to five times their original length, which ensured the orientation of the two-dimensional nanofillers. Finally the films were annealed at  $120$  °C. Unlike the nanocomposites filled with high- $K$  materials, the P(VDF-HFP)–kaolinite clay nanocomposites exhibited decreased loss with increasing filler content, as proved in both the weak field (dielectric spectroscopy) and high field measurements ( $D$ - $E$  loop) (Fig. 6.13).

In the meantime, the electric displacement decreased significantly in the nanocomposites compared with that of the blank polymer. Two mechanisms were proposed to rationalize the origin of this trend. First, two-dimensional nanofillers serve as nucleating agents to promote growth of nonpolar crystals in their vicinity. Due to the restricted mobility of the dipoles in these crystals, their reorientation requires higher electric fields. Second, oriented dipole density is reduced because of the incorporation of inorganic fillers, which in turn leads to a lower amount of space charge required for polarization stabilization. The high aspect ratio two-dimensional nanofillers also build up efficient conduction barriers that can limit the charge migration toward the electrodes and hinder the electrical tree growth during breakdown. These aspects contribute to the significantly improved breakdown strength of the nanocomposites, and as such, the discharged energy density increased by  $100\%$  relative to the blank polymer despite of the reduced electric displacement. Similar results were observed using other nanolaminate fillers such as montmorillonites, and filler orientation was found to be able to provide more ordered trapping centers to obstruct the ability of charges to traverse the sample to the opposite electrode [102, 103].



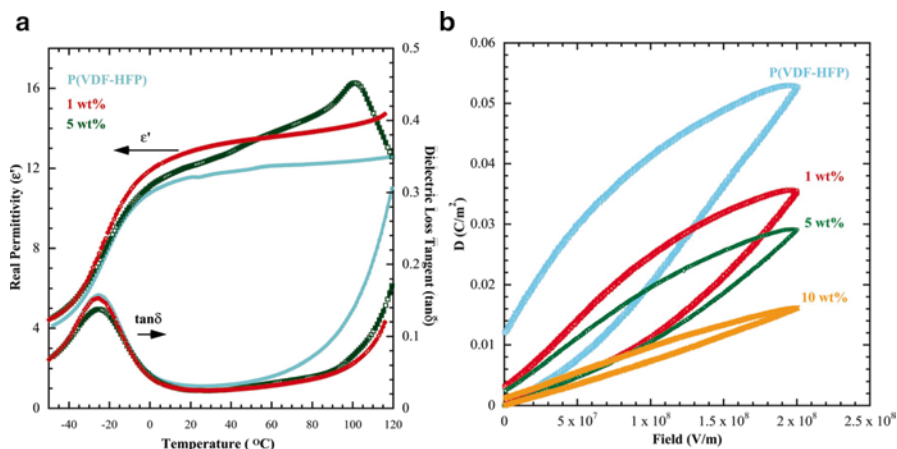


**Fig. 6.13** (a) Dielectric permittivity and dielectric loss tangent vs. temperature, at low electric field and 1 kHz, for the stretched films of unfilled P(VDF-HFP) and two nanocomposites with 1 and 5 wt. % kaolinite. (b) Displacement vs. electric field loops of P(VDF-HFP) and its nanocomposites; all films were uniaxially stretched. Upon kaolinite filler addition, there is a systematic reduction in remnant polarization and an associated improvement in losses (Reprinted from Ref. [101] with permission from AIP Publishing LLC)

## 6.4 Simultaneous Improvements of Dielectric Constant and Breakdown Strength

It is envisaged that the integration of complementary elements such as large dielectric constant from ceramics and high breakdown strength from polymers in the polymer nanocomposites could lead to an enhanced energy storage capacity. However, it remains elusive how the contradictory criteria of enhancing one parameter while maintaining the other could be balanced in the nanocomposites. For example, a marked decrease in  $E_b$  due to a large contrast in  $K$  between ceramics and polymers, as shown in current high- $K$  filler involved dielectric nanocomposites, negates any potential substantial increase in energy density under high electric fields. In this regard, the ideal case would be simultaneous improvements of dielectric constant and breakdown strength in the nanocomposites.

This was achieved recently by employing multicomponent filler systems and utilizing either topological-structure or interface engineering [104, 105]. Shen and colleagues expanded the traditional 0-3 nanocomposite system to a multilayered structure fabricated through a simple layer-by-layer tape casting method (Fig. 6.14) [104]. For instance, they demonstrated a 3-layer structure, in which a center layer was designed to be a nanocomposite with higher breakdown strength and the top and bottom layers were both nanocomposites with high dielectric constants. Therefore, the center layer was able to improve the overall breakdown strength of the multilayer-structured nanocomposite, while the outer layers enhanced the electric displacement. As a result, the topological-structured nano-

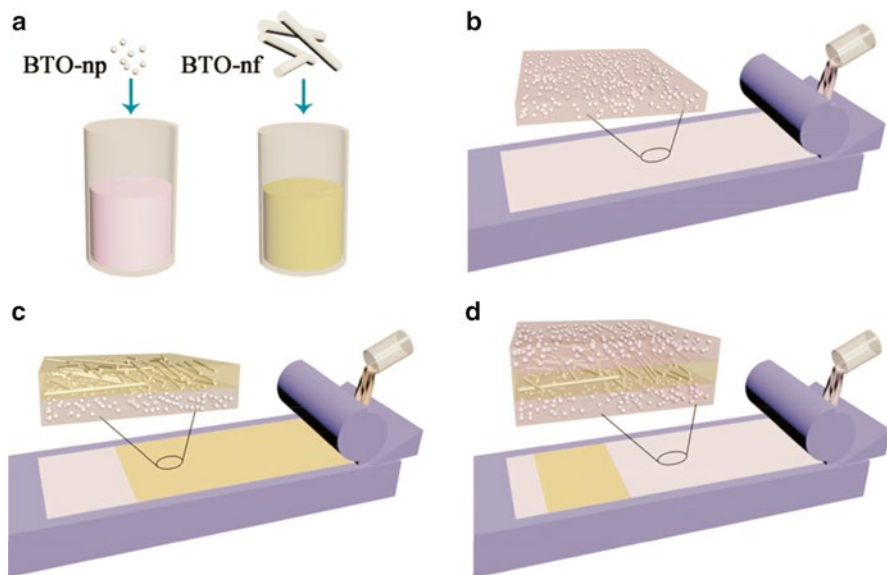


**Fig. 6.14** Schematic drawing of the approach of layer-by-layer casting for the fabrication of the sandwich multilayer films. (a) Nanofillers were dispersed in the PVDF suspension, (b) one layer with BTO-np was cast, (c) the central layer with BTO-nf was cast, (d) the other layer with BTO-np was cast (Reprinted from Ref. [104] with permission from John Wiley and Sons)

composites were found to show much improved capacitive energy storage performance than the matrix polymer, i.e., a 162 % increase in discharged energy density, which was resulted from the simultaneous improvements of dielectric constant (from 7 to 10) and breakdown strength (from 260 to 450 kV/mm) in the nanocomposite. This approach combines the complementary properties of the constituent layers and thus leads to superior material performance than using traditional nanocomposite systems.

More recently, Shen and colleagues developed another approach to simultaneously improving dielectric constant and breakdown strength in polymer nanocomposites (Fig. 6.15) [105]. They employed a new type of material, i.e.,  $\text{BaTiO}_3\text{-TiO}_2$  nanofibers, where  $\text{BaTiO}_3$  nanoparticles are embedded in  $\text{TiO}_2$  nanofibers as inclusions in PVDF-based polymer nanocomposites. The discharged energy density of the nanocomposite was reported to be as high as  $20 \text{ J/cm}^3$ , which was from the increased electric displacement (72 % increment) and characteristic breakdown strength (8 % increment). While the origin of the increase in breakdown strength was claimed to be the large aspect ratio and partial orientation of nanofibers, the improvement in electric displacement was ascribed to the interfacial effect inside the integrated nanofillers. This was supported by the evidence from simulated atomic-resolution angular bright-field images, from which a clear interfacial layer could be observed at the intermediate region between the embedded  $\text{BaTiO}_3$  nanoparticles and the host  $\text{TiO}_2$  nanofiber. Such interfacial layer possessed a different lattice structure to those of the  $\text{BaTiO}_3$  and  $\text{TiO}_2$  phases. The interpretation made

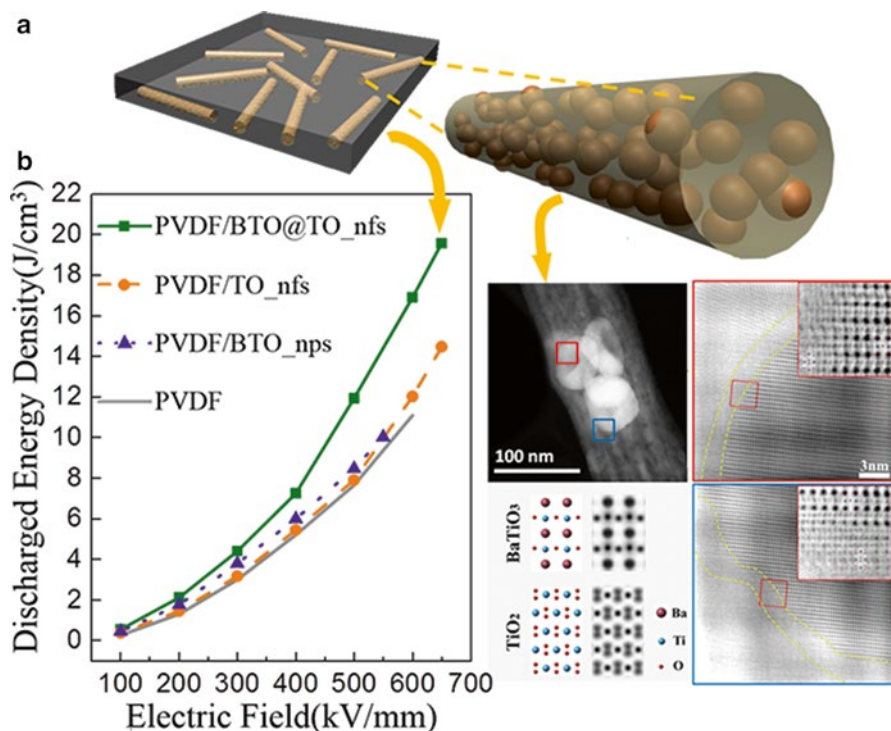


**Fig. 6.15** (a) Schematic illustration of BTO@TO\_nfs and PVDF-BTO@TO\_nfs nanocomposites. (b) Discharged energy density of PVDF nanocomposites embedded with BTO@TO\_nfs, TO\_nfs, BTO\_nps, and pure PVDF films as a function of electric field, the volume fraction of the three nano-inclusions were fixed at 3 % in all composites. (c) Structural models of BaTiO<sub>3</sub> and TiO<sub>2</sub> and corresponding simulated atomic-resolution angular bright-field images (Reprinted from Ref. [105] with permission from John Wiley and Sons)

on the basis of this observation was the Ba–Ti mutual occupation at the intermediate regions between BaTiO<sub>3</sub> and TiO<sub>2</sub> and thus a large strain should exist in these regions to benefit polarization. This work revealed that, in addition to the interfacial polarization between the inorganic fillers and the polymer matrices, the interfacial effect inside hierarchical multiphase inorganic inclusions could also significantly affect dielectric properties of polymer nanocomposites and therefore be employed to achieve high energy density in dielectric capacitors.

## 6.5 Conclusions

Recent advances in nanomaterials and nanotechnology have propelled the development of dielectric polymer nanocomposites. The state-of-the-art energy density attained in polymer nanocomposites has already exceeded 20 J/cm<sup>3</sup>, which is comparable to those of commercially available electrochemical capacitors. However,

this is far from the end of story as the performance still fall well short of the needs in applications such as electric drive vehicles, pulsed power, and power capacitors, which require not only high energy and power densities but also low loss. It is worth pointing out that while tremendous efforts have been placed on the search for new nano-inclusions with tailored morphologies and electrical properties, minor progress has been gained on the exploitation of high- $K$  polymers. Note that a majority of achievements made on high-energy-density polymer nanocomposites are still employing PVDF-based polymers as the host matrix that has been studied over decades. Unfortunately, PVDF-based polymers have high loss values, i.e.,  $>3\%$  under weak electric fields and could be over  $50\%$  under high electric fields, which is unaccepted for many of the proposed applications. This is somewhat related to the low glass transition temperatures, low Curie temperatures, and low melting points of PVDF-based polymers. On the other hand, the current high-energy-density polymer nanocomposites are exclusively designed for room temperature applications due to the limitation in thermal stabilities of existing high- $K$  polymers and are not suitable for harsh condition operations commonly presented in the emerging applications such as electric drive vehicles and deep oil and gas explorations. These concerns raise new challenges in designing the next generation organic capacitor dielectrics. Besides, in-depth knowledge about the matrix–filler coupling effect in dielectric polymer nanocomposites is highly demanded to assist the material selection and engineering as it contributes a major part to the dielectric polarization that defines the energy density. Fundamental understanding of electrical conduction mechanisms in dielectric polymer nanocomposites could help with the optimization of material design, fabrication, and processing in a way high efficiency charge–discharge could be attained. Last but not least, breakthrough could also be made through new designs of composition and structure of polymer nanocomposites. The multilayer-structured polymer nanocomposites proposed by Shen et al. (ref. [104]) stands for a good example along this direction. Multifunctional filler systems may also deserve attentions to realize promoted collective performance. All these efforts together would push this interdisciplinary field onto a new stage to match the needs for electricity in future transportations, portable electronic devices, and storage and conversion of renewable energy sources.

## References

1. Pikul JH, Zhang HG, Cho J, Braun PV, King WP (2013) High-power lithium ion microbatteries from interdigitated three-dimensional bicontinuous nanoporous electrodes. *Nat Commun* 4:1732
2. El-Kady MF, Strong V, Dubin S, Kaner RB (2012) Laser scribing of high-performance and flexible graphene-based electrochemical capacitors. *Science* 335:1326–1330
3. Wu ZS, Parves K, Feng XL, Müllen K (2013) Graphene-based in-plane micro-supercapacitors with high power and energy densities. *Nat Commun* 4:2487
4. Burke A (2007) R&D considerations for the performance and application of electrochemical capacitors. *Electrochim Acta* 53:1083–1091

5. Dang ZM, Wu JB, Fan LZ, Nan CW (2003) Dielectric behavior of Li and Ti co-doped NiO/PVDF composites. *Chem Phys Lett* 376:389–394
6. Subodh G, Deepu V, Mohanan P, Sebastian MT (2009) Dielectric response of high permittivity polymer ceramic composite with low loss tangent. *Appl Phys Lett* 95:062903
7. Zhou X, Zhao XH, Suo ZG, Zou C, Runt J, Liu S, Zhang SH, Zhang QM (2009) Electrical breakdown and ultrahigh electrical energy density in poly(vinylidene fluoride-hexafluoropropylene) copolymer. *Appl Phys Lett* 94:162901
8. Parvatikar N, Ambika Prasad MVN (2006) Frequency-dependent conductivity and dielectric permittivity of polyaniline/CeO<sub>2</sub> composites. *J Appl Polym Sci* 100:1403–1405
9. Afzal AB, Akhtar MJ, Nadeem M, Hassan MM (2009) Investigation of structural and electrical properties of polyaniline/gold nanocomposites. *J Phys Chem C* 113:17560–17565
10. Schroeder R, Majewski LA, Grell M (2005) High-performance organic transistors using solution-processed nanoparticle-filled high-*k* polymer gate insulators. *Adv Mater* 17:1535–1539
11. Ginzburg VV, Myers K, Malowinski S, Cieslinski R, Elwell M, Bernius M (2006) High-dielectric-constant self-assembled nodular structures in polymer/gold nanoparticle films. *Macromolecules* 39:3901–3906
12. Guo N, DiBenedetto SA, Tewari P, Lanagan MT, Ratner MA, Marks TJ (2010) Nanoparticle, size, shape, and interfacial effects on leakage current density, permittivity, and breakdown strength of metal oxide–polyolefin nanocomposites: experiment and theory. *Chem Mater* 22:1567–1578
13. Love GR (1990) Energy storage in ceramic dielectric. *J Am Ceram Soc* 73:323–328
14. Cao Y, Irwin PC, Younsi K (2004) The future of nanodielectrics in the electric power industry. *IEEE Trans Dielectr Electr Insul* 11:797–807
15. Rabuffi M, Picci G (2002) Status quo and future prospects for metallized polypropylene energy storage capacitors. *IEEE Trans Plasma Sci* 30:1939–1942
16. Chu BJ, Zhou X, Ren KL, Neese B, Lin MR, Wang Q, Bauer F, Zhang QM (2006) A dielectric polymer with high electric energy density and fast discharge speed. *Science* 313:334–336
17. Ho J, Jow TR (2012) High field conduction in biaxially oriented polypropylene at elevated temperature. *IEEE Trans Dielectr Electr Insul* 19:990–995
18. Levy O, Stroud D (1997) Maxwell Garnett theory for mixtures of anisotropic inclusions: application to conducting polymers. *Phys Rev B* 56:8035
19. Nan CW, Shen Y, Ma J (2010) Physical properties of composites near percolation. *Annu Rev Mater Res* 40:131
20. Wang Q, Zhu L (2011) Polymer nanocomposites for electrical energy storage. *J Polym Sci B Polym Phys* 49:1421–1429
21. Dang ZM, Yuan JK, Yao SH, Liao RJ (2013) Flexible nanodielectric materials with high permittivity for power energy storage. *Adv Mater* 25:6334–6365
22. Li J, Seok SI, Chu B, Dogan F, Zhang Q, Wang Q (2009) Nanocomposites of ferroelectric polymers with TiO<sub>2</sub> nanoparticles exhibiting significantly enhanced electrical energy density. *Adv Mater* 21:217
23. Li J, Claude J, Norena-Franco LE, Il Seok S, Wang Q (2008) Electrical energy storage in ferroelectric polymer nanocomposites containing surface-functionalized BaTiO<sub>3</sub> nanoparticles. *Chem Mater* 20:6304
24. Kim P, Doss NM, Tillotson JP, Hotchkiss PJ, Pan MJ, Marder SR, Li J, Calame JP, Perry JW (2009) High energy density nanocomposites based on surface-modified BaTiO<sub>3</sub> and a ferroelectric polymer. *ACS Nano* 3:2581
25. Kim P, Jones SC, Hotchkiss PJ, Haddock JN, Kippelen B, Marder SR, Perry JW (2007) Phosphonic acid-modified barium titanate polymer nanocomposites with high permittivity and dielectric strength. *Adv Mater* 19:1001–1005
26. Li Z, Fredin LA, Tewari P, DiBenedetto SA, Lanagan MT, Ratner MA, Marks TJ (2010) In situ catalytic encapsulation of core-shell nanoparticles having variable shell thickness:

- dielectric and energy storage properties of high-permittivity metal oxide nanocomposites. *Chem Mater* 22:5154
27. Li J, Khanchaitit P, Han K, Wang Q (2010) New route toward high-energy-density nanocomposites based on chain-end functionalized ferroelectric polymers. *Chem Mater* 22:5350
  28. Deng Y, Zhang Y, Xiang Y, Wang G, Xu H (2009)  $\text{Bi}_2\text{S}_3$ - $\text{BaTiO}_3$ /PVDF three-phase composites with high dielectric permittivity. *J Mater Chem* 19:2058
  29. Huang X, Xie L, Jiang P, Wang G, Liu F (2009) Electrical, thermophysical and micromechanical properties of ethylene-vinyl acetate elastomer composites with surface modified  $\text{BaTiO}_3$  nanoparticles. *J Phys D Appl Phys* 42:245407
  30. Jung HM, Kang JH, Yang SY, Won JC, Kim YS (2010) Barium titanate nanoparticles with diblock copolymer shielding layers for high-energy density nanocomposites. *Chem Mater* 22:450
  31. Dang ZM, Wang HY, Xu HP (2006) Influence of silane coupling agent on morphology and dielectric property in  $\text{BaTiO}_3$ /polyvinylidene fluoride composites. *Appl Phys Lett* 89:112902
  32. Song Y, Shen Y, Liu H, Lin Y, Li M, Nan CW (2012) Enhanced dielectric and ferroelectric properties induced by dopamine-modified  $\text{BaTiO}_3$  nanofibers in flexible poly(vinylidene fluoride-trifluoroethylene) nanocomposites. *J Mater Chem* 22:8063
  33. Song Y, Shen Y, Liu H, Lin Y, Li M, Nan CW (2012) Improving the dielectric constants and breakdown strength of polymer composites: effects of the shape of the  $\text{BaTiO}_3$  nano-inclusions, surface modification and polymer matrix. *J Mater Chem* 22:16491
  34. Tuncer E, Sauers I, James DR, Duckworth RC (2008) Electrical properties of percolative polystyrene/carbon nanofiber composites. *IEEE Trans Dielectr Electr Insul* 15:236
  35. Dou XL, Liu XL, Zhang Y, Feng H, Chen JF, Du S (2009) Improved dielectric strength of barium titanate-polyvinylidene fluoride nanocomposite. *Appl Phys Lett* 95:132904
  36. Dang ZM, Zhou T, Yao SH, Yuan JK, Zha JW, Song HT, Li JY, Chen Q, Yang WT, Bai J (2009) Advanced calcium copper titanate/polyimide functional hybrid films with high dielectric permittivity. *Adv Mater* 21:2077
  37. Yang W, Yu S, Sun R, Du R (2011) Nano- and microsize effect of CCTO fillers on the dielectric behavior of CCTO/PVDF composites. *Acta Mater* 59:5593
  38. Prakash BS, Varma KBR (2007) Dielectric behavior of CCTO/epoxy and Al-CCTO/epoxy composites. *Compos Sci Technol* 67:2363
  39. Amaral F, Rubinger CPL, Henry F, Costa LC, Valente MA, Barros-Timmons A (2008) Dielectric properties of polystyrene-CCTO composite. *J Non Cryst Solids* 354:5321
  40. Tang HX, Lin YR, Andrews C, Sodano HA (2011) Nanocomposites with increased energy density through high aspect ratio PZT nanowires. *Nanotechnology* 22:015702
  41. Yao J, Xiong C, Dong L, Chen C, Lei Y, Chen L, Li R, Zhu Q, Liu X (2009) Enhancement of dielectric constant and piezoelectric coefficient of ceramic-polymer composites by interface chelation. *J Mater Chem* 19:2817
  42. Banerjee S, Cook-Chennault KA (2011) Influence of Al particle size and lead zirconate titanate (PZT) volume fraction on the dielectric properties of PZT-epoxy-aluminum composites. *J Eng Mater Technol* 133:041016
  43. Tang H, Lin Y, Sodano HA (2012) Enhanced energy storage in nanocomposite capacitors through aligned PZT nanowires by uniaxial strain assembly. *Adv Energy Mater* 2:469
  44. Yu K, Wang H, Zhou Y, Bai Y, Niu Y (2013) Enhanced dielectric properties of  $\text{BaTiO}_3$ /poly(vinylidene fluoride) nanocomposites for energy storage applications. *J Appl Phys* 113:034105
  45. Tomer V, Polizos G, Manias E, Randall CA (2010) Epoxy-based nanocomposites for electrical energy storage. I: effects of montmorillonite and barium titanate nanofillers. *J Appl Phys* 108:074116
  46. Xia WM, Xu Z, Wen F, Zhang ZC (2012) Electrical energy density and dielectric properties of poly(vinylidene fluoride-chlorotrifluoroethylene)/ $\text{BaSrTiO}_3$  nanocomposites. *Ceram Int* 38:1071-1075
  47. Ducharme S (2009) An inside-out approach to storing electrostatic energy. *ACS Nano* 3:2447

48. Guo N, DiBenedetto SA, Kwon DK, Wang L, Russell MT, Lanagan MT, Facchetti A, Marks TJ (2007) Supported metallocene catalysis for in situ synthesis of high energy density metal oxide nanocomposites. *J Am Chem Soc* 129:766
49. Xie L, Huang X, Wu C, Jiang P (2011) Core-shell structured poly(methyl methacrylate)/BaTiO<sub>3</sub> nanocomposites prepared by in situ atom transfer radical polymerization: a route to high dielectric constant materials with the inherent low loss of the base polymer. *J Mater Chem* 21:5897
50. Paniagua SA, Kim YS, Henry K, Kumar R, Perry JW, Marder SR (2014) Surface-initiated polymerization from barium titanate nanoparticles for hybrid dielectric capacitors. *ACS Appl Mater Interfaces* 6:3477
51. Yang K, Huang XY, Xie LY, Wu C, Jiang PK, Tanaka T (2012) Core-shell structured polystyrene/BaTiO<sub>3</sub> hybrid nanodielectrics prepared by in situ RAFT polymerization: a route to high dielectric constant and low loss materials with weak frequency dependence. *Macromol Rapid Comm* 33:1921
52. Xie LY, Huang XY, Yang K, Li ST, Jiang PK (2014) "Grafting to" route to PVDF-HFP-GMA/BaTiO<sub>3</sub> nanocomposites with high dielectric constant and high thermal conductivity for energy storage and thermal management applications. *J Mater Chem A* 2:5244–5251
53. Tchoul MN, Fillery SP, Koerner H, Drummy LF, Oyerokun FT, Mirau PA, Durstock MF, Vaia RA (2010) Assemblies of titanium dioxide-polystyrene hybrid nanoparticles for dielectric applications. *Chem Mater* 22:1749
54. Maliakal A, Katz H, Cotts P, Subramoney S, Mirau P (2005) Inorganic oxide core, polymer shell nanocomposite as a high K gate dielectric for flexible electronics applications. *J Am Chem Soc* 127:14655
55. Tang HX, Lin YR, Sodano HA (2013) Synthesis of high aspect ratio BaTiO<sub>3</sub> nanowires for high energy density nanocomposite capacitors. *Adv Energy Mater* 3:451–456
56. Tang HX, Sodano HA (2013) Ultra high energy density nanocomposite capacitors with fast discharge using Ba<sub>0.2</sub>Sr<sub>0.8</sub>TiO<sub>3</sub> nanowires. *Nano Lett* 13:1373–1379
57. Tang HX, Sodano HA (2013) High energy density nanocomposite capacitors using non-ferroelectric nanowires. *Appl Phys Lett* 102:063901
58. Zhou Z, Tang HX, Lin YR, Sodano HA (2013) Hydrothermal growth of textured Ba<sub>x</sub>Sr<sub>1-x</sub>TiO<sub>3</sub> films composed of nanowires. *Nanoscale* 5:10901–10907
59. Zou C, Kushner D, Zhang S (2011) Wide temperature polyimide/ZrO<sub>2</sub> polyimide/ZrO<sub>2</sub> nanodielectric capacitor film with excellent electrical performance. *Appl Phys Lett* 98:082905
60. Balasubramanian B, Kraemer KL, Reding NA, Skomski R, Ducharme S, Sellmyer DJ (2010) Synthesis of monodisperse TiO<sub>2</sub>-paraffin core-shell nanoparticles for improved dielectric properties. *ACS Nano* 4:1893
61. Lin S, Kuang X, Wang F, Zhu H (2012) Effect of TiO<sub>2</sub> crystalline composition on the dielectric properties of TiO<sub>2</sub>/P(VDF-TrFE) composites. *Phys Status Solidi RRL* 6:352
62. Ouyang G, Wang K, Chen XY (2012) TiO<sub>2</sub> nanoparticles modified polydimethylsiloxane with fast response time and increased dielectric constant. *J Micromech Microeng* 22:074002
63. Dang ZM, Xia YJ, Zha JW, Yuan JK, Bai J (2011) Preparation and dielectric properties of surface modified TiO<sub>2</sub>/silicone rubber nanocomposites. *Mater Lett* 65:3430
64. Zha JW, Dang ZM, Zhou T, Song HT, Chen G (2010) Electrical properties of TiO<sub>2</sub>-filled polyimide nanocomposite films prepared via an in situ polymerization process. *Synth Met* 160:2670
65. Zha JW, Fan BH, Dang ZM, Li ST, Chen G (2010) Microstructure and electrical properties in three-component (Al<sub>2</sub>O<sub>3</sub>-TiO<sub>2</sub>)/polyimide nanocomposite films. *J Mater Res* 25:2384
66. McCarthy DN, Stoyanov H, Rychkov D, Ragusch H, Melzer M, Kofod G (2012) Increased permittivity nanocomposite dielectrics by controlled interfacial interactions. *Compos Sci Technol* 72:731
67. Nan CW (1993) Physics of inhomogeneous inorganic materials. *Prog Mater Sci* 37:1
68. Huang XY, Jiang PK, Kim CU (2007) Electrical properties of polyethylene/aluminum nanocomposites. *J Appl Phys* 102:124103

69. Panda M, Srinivas V, Thakur AK (2011) Role of polymer matrix in large enhancement of dielectric constant in polymer-metal composites. *Appl Phys Lett* 99:042905
70. Dang ZM, Lin YH, Nan CW (2003) Novel ferroelectric polymer composites with high dielectric constants. *Adv Mater* 15:1625
71. Panda M, Srinivas V, Thakur AK (2008) On the question of percolation threshold in polyvinylidene fluoride/nanocrystalline nickel composites. *Appl Phys Lett* 92:132905
72. Huang XY, Jiang PK, Xie LY (2009) Ferroelectric polymer/silver nanocomposites with high dielectric constant and high thermal conductivity. *Appl Phys Lett* 95:242901
73. Panda M, Srinivas V, Thakur AK (2008) Surface and interfacial effect of filler particle on electrical properties of polyvinylidene fluoride/nickel composites. *Appl Phys Lett* 93:242908
74. Kofod G, Risse S, Stoyanov H, McCarthy DN, Sokolov S, Kraehnert R (2011) Broad-spectrum enhancement of polymer composite dielectric constant at ultralow volume fractions of silica-supported copper nanoparticles. *ACS Nano* 5:1623
75. Shen Y, Lin YH, Li M, Nan CW (2007) High dielectric performance of polymer composite films induced by a percolating interparticle barrier layer. *Adv Mater* 19:1418–1422
76. Fredin LA, Li Z, Lanagan MT, Ratner MA, Marks TJ (2013) Substantial recoverable energy storage in percolative metallic aluminum-polypropylene nanocomposites. *Adv Funct Mater* 23:3560–3569
77. Yao SH, Dang ZM, Jiang MJ, Xu HP, Bai JB (2007) Influence of aspect ratio of carbon nanotube on percolation threshold in ferroelectric polymer nanocomposite. *Appl Phys Lett* 91:212901
78. Dang ZM, Wang L, Yin Y, Zhang Q, Lei QQ (2007) Giant dielectric permittivities in functionalized carbon-nanotube/electroactive-polymer nanocomposites. *Adv Mater* 19:852
79. Wang L, Dang ZM (2005) Carbon nanotube composites with high dielectric constant at low percolation threshold. *Appl Phys Lett* 87:042903
80. Li Q, Xue QZ, Hao LZ, Gao XL, Zheng QB (2008) Large dielectric constant of the chemically functionalized carbon nanotube/polymer composites. *Compos Sci Technol* 68:2290
81. Yao SH, Dang ZM, Xu HP, Jiang MJ, Bai J (2008) Exploration of dielectric constant dependence on evolution of microstructure in nanotube/ferroelectric polymer nanocomposites. *Appl Phys Lett* 92:082902
82. Chang J, Liang G, Gu A, Cai S, Yuan L (2012) The production of carbon nanotube/epoxy composites with a very high dielectric constant and low dielectric loss by microwave curing. *Carbon* 50:689
83. Simoes R, Silva J, Vaia R, Sencadas V, Costa P, Gomes J, Lanceros-Mendez S (2009) Low percolation transitions in carbon nanotube networks dispersed in a polymer matrix: dielectric properties, simulations and experiments. *Nanotechnology* 20:035703
84. Yuan JK, Yao SH, Sylvestre A, Bai J (2012) Biphasic polymer blends containing carbon nanotubes: heterogeneous nanotube distribution and its influence on the dielectric properties. *J Phys Chem C* 116:2051
85. Yuan JK, Yao SH, Dang ZM, Sylvestre A, Genestoux M, Bai J (2011) Giant dielectric permittivity nanocomposites: realizing true potential of pristine carbon nanotubes in polyvinylidene fluoride matrix through an enhanced interfacial interaction. *J Phys Chem C* 115:5515
86. Yuan JK, Li WL, Yao SH, Lin YQ, Sylvestre A, Bai J (2011) High dielectric permittivity and low percolation threshold in polymer composites based on SiC-carbon nanotubes micro/nano hybrid. *Appl Phys Lett* 98:032901
87. Zhang S, Wang H, Wang G, Jiang Z (2012) Material with high dielectric constant, low dielectric loss, and good mechanical and thermal properties produced using multi-wall carbon nanotubes wrapped with poly(ether sulphone) in a poly(ether ether ketone) matrix. *Appl Phys Lett* 101:012904
88. Wu C, Huang X, Wu X, Yu J, Xie L, Jiang P (2012) TiO<sub>2</sub>-nanorod decorated carbon nanotubes for high-permittivity and low-dielectric-loss polystyrene composites. *Compos Sci Technol* 72:521



89. Sun LL, Li B, Zhao Y, Mitchell G, Zhong WH (2010) Structure-induced high dielectric constant and low loss of CNF/PVDF composites with heterogeneous CNF distribution. *Nanotechnology* 21:305702
90. Sun LL, Zhao Y, Zhong WH (2011) Dependence of dielectric properties and percolative behavior on phase separation structure induced by heterogeneous carbon nanofiber distribution in polymer blend nanocomposites. *Macromol Mater Eng* 296:992
91. Barick AK, Tripathy DK (2012) Preparation and characterization of carbon nanofiber reinforced thermoplastic polyurethane nanocomposites. *J Appl Polym Sci* 124:765
92. Sun LL, Zhang ZG, Zhong WH (2011) Fluorination deposition on carbon nanofibers by PTFE decomposition as a facile method to enhance dispersion and interaction in PVDF composites. *J Mater Chem* 21:944
93. He F, Lau S, Chan HL, Fan JT (2009) High dielectric permittivity and low percolation threshold in nanocomposites based on poly(vinylidene fluoride) and exfoliated graphite nanoplates. *Adv Mater* 21:710
94. Yu J, Huang X, Wu C, Jiang P (2011) Permittivity, thermal conductivity and thermal stability of poly(vinylidene fluoride)/graphene nanocomposites. *IEEE Trans Dielectr Electr Insul* 18:478
95. Han K, Li Q, Chen ZY, Gadinski MR, Dong LJ, Xiong CX, Wang Q (2013) Suppression of energy dissipation and enhancement of breakdown strength in ferroelectric polymer-graphene percolative composites. *J Mater Chem C* 1:7034–7042
96. Fan P, Wang L, Yang J, Chen F, Zhong M (2012) Graphene/poly(vinylidene fluoride) composites with high dielectric constant and low percolation threshold. *Nanotechnology* 23:365702
97. Wu C, Huang X, Wang G, Wu X, Yang K, Li S, Jiang P (2012) Hyperbranched-polymer functionalization of graphene sheets for enhanced mechanical and dielectric properties of polyurethane composites. *J Mater Chem* 22:7010
98. Wang DR, Bao YR, Zha JW, Zhao J, Dang ZM, Hu GH (2012) Improved dielectric properties of nanocomposites based on poly(vinylidene fluoride) and poly(vinyl alcohol)-functionalized graphene. *ACS Appl Mater Interfaces* 4:6273–6279
99. Roy M, Nelson JK, McCrone RK, Schadler LS, Reed CW, Keefe R, Zeneger W (2005) Polymer nanocomposite dielectrics—the role of the interface. *IEEE Trans Dielectr Electr Insul* 12:629–643
100. Takala M, Ranta H, Nevalainen P, Pakonen P, Pelto J, Karttunen M, Virtanen S, Koivu V, Pettersson M, Sonerud B, Kannus K (2010) Dielectric properties and partial discharge endurance of polypropylene-silica nanocomposite. *IEEE Trans Dielectr Electr Insul* 17:1259–1267
101. Tomer V, Manias E, Randall CA (2011) High field properties and energy storage in nanocomposite dielectrics of poly(vinylidene fluoride-hexafluoropropylene). *J Appl Phys* 110:044107
102. Tomer V, Polizos G, Randall CA, Manias E (2011) Polyethylene nanocomposite dielectrics: implications of nanofiller orientation on high field properties and energy storage. *J Appl Phys* 109:074113
103. Fillery SP, Koerner H, Drummy L, Dunkerley E, Durstock MF, Schmidt DF, Vaia RA (2012) Nanolaminates: increasing dielectric breakdown strength of composites. *ACS Appl Mater Interfaces* 4:1388–1396
104. Hu PH, Shen Y, Guan YH, Zhang XH, Lin YH, Zhang QM, Nan CW (2014) Topological-structure modulated polymer nanocomposites exhibiting highly enhanced dielectric strength and energy density. *Adv Funct Mater* 24:3172–3178
105. Zhang X, Shen Y, Zhang QH, Gu L, Hu YH, Du JW, Lin YH, Nan CW (2015) Ultrahigh energy density of polymer nanocomposites containing BaTiO<sub>3</sub>@TiO<sub>2</sub> nanofibers by atomic-scale interface engineering. *Adv Mater* 27:819–824